Published in final edited form as:
Carbon N Y. 2018 ; 129: 137–151. doi:10.1016/j.carbon.2017.10.038.

Environmental aging and degradation of multiwalled carbon nanotube reinforced polypropylene

Changseok Han[a], **Endalkachew Sahle-Demessie**[b,*], **Amy Q. Zhao**[b], **Teri Richardson**[b], **Jun Wang**[c]

[a]Oak Ridge Institute for Science and Education, Oak Ridge, TN 37831, USA

[b]U.S. Environmental Protection Agency, Office of Research and Development, National Risk Management Laboratory, 26 W. Martin Luther King Drive, Cincinnati, OH 45268, USA

[c]Perkin Elmer, Inc., 710 Bridgeport Avenue, Shelton, CT 06484-4794, USA

Abstract

The degradation of polypropylene (PP) and PP-multiwalled carbon nanotube (PP-MWCNT) panels during environmental weathering resulted in an increased degree of crystallinity, making them brittle, and creating surface cracks. The degradation led to a breakdown of the panels and increased the potential for nanorelease. Thermal analysis revealed that the thickness of the test panels and reinforcement with MWCNTs had a significant influence on the stability of PP-MWCNT composites. Differential scanning calorimetry indicated that the MWCNTs acted as nucleation points, increasing the crystallization temperatures of PP-MWCNT, which reduced the extent of aging. Weathering decreased both the melting and crystallization temperatures of PP by as much as 20 o C. The reduction in the temperatures was inversely proportional to the thickness of the panels. The activation energy (E_a) obtained using isoconversional kinetics of the TGA analysis showed that the effective thermo-oxidative degradations of PP changed during aging. The E_a for the initial stages of thermal degradation decreased from ~330 kJ/mol to ~100 kJ/mol for aged PP. During the late degradation stages, the E_a values increased to ~300 kJ/mol. These results suggest that early degradation were altered because of the changes in the molecular structure of the aged P and a shift in the degradation rate-limiting steps.

Graphical Abstract

*Corresponding author.

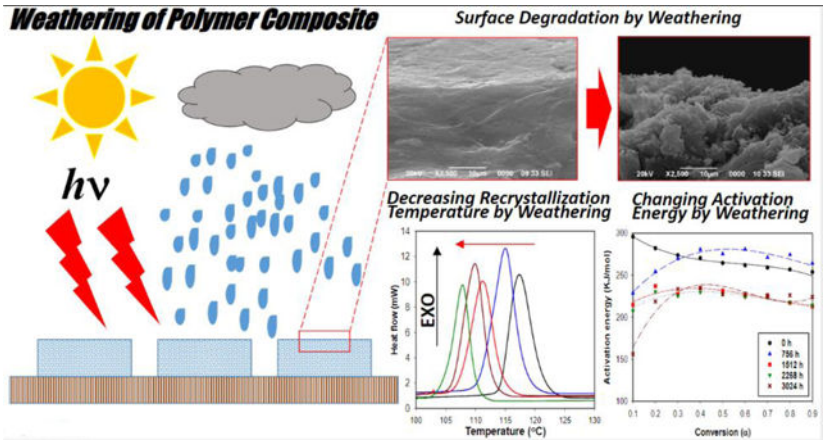

Keywords

Polypropylene MWCNT; Weathering Activation energy; Melting-crystallization points

1. Introduction

Polymer composites that are reinforced with carbon nanotubes (CNT) show enhanced mechanical and physical matrix properties. The broad spectrum uses of these CNT/polymer composites for industrial applications, and consumer use, may lead to unintended contamination of land or aquatic ecosystems and increased risks of exposure to humans and the environment. However, there are a limited number of studies on the aging of different nanocomposites and the potential release of embedded filler materials due to environmental aging. Polypropylene (PP) was selected for this study since it is a thermoplastic commonly used for a broad range of applications such as automotive parts, food packaging, housing materials and electrical devices. PP is a semi-crystalline general-purpose polymer that is inexpensive, and is highly mechanically robust with high resistance to water and chemicals [1–4]. Nanomaterials have been widely incorporated into polymers to improve the physicochemical properties or provide multi-functions to pristine polymers. Among nanomaterials, multiwalled carbon nanotubes (MWCNTs) have been intensively used as an additive to the plastic to make lighter and stronger materials with higher thermal stability and water resistance [5–9]. Because single- or multi-walled carbon nanotubes are approximately the same length as polymer chain-segments, the interaction and mobility result in a marked increase in physical and mechanical properties.

Although nano-reinforcement improves the properties of polymers, added MWCNTs could be released into the environment as composites age, or due to mechanical defects during production, usage phase or at the end of their use. The toxicity of MWCNTs to human and animal cells and microorganisms has been related to the formation of reactive oxygen species. However, the 50% lethal concentration (LC_{50}) has rarely been discussed since MWCNTs have diverse physicochemical and toxic properties [10–12]. Studies have shown that micro- and nanomaterials are traps for persistent organic pollutants (POPs) in the environment. The interaction of released MWCNTs with organic pollutants in the

environment can alter the fate and transport of hydrophobic persistent organic pollutants (POPs) [13,14]. A recent study indicated that MWCNTs released into aquatic environment adsorbed hydrophobic organic contaminants, including pesticides and polyaromatic hydrocarbons (PAHs). Debris of micro-polymers and released nanomaterials accumulate POPs and increased the availability of contaminants in water phase by order of magnitude [14], Therefore, there is a need to study the stability and degradation of nanocomposites by environmental aging (e.g., photooxidation, chemical oxidation, and mechanical abrasion) for understanding the risk of released of nanomaterials from polymer nanocomposites better.

Several reports have indicated increased thermal stability in nanotube-polymer composites [2,4,6]. However, environmental aging may alter the structural, physical and chemical properties of the nanocomposite, which are associated with the stability and degradation of nanocomposites and potential release of nanoadditives. Although long-term tests under natural service conditions represent real conditions, accelerated aging tests are carried out to investigate a conveniently short time relative ranking of the chemical stability or physical durability of materials. Accelerated aging tests simulate weather conditions, including sunny and rainy days following pre-selected cycles. These tests are used to estimate, or "predict," potential long-term serviceability of material and to elucidate the chemical reactions involved the consequences of releasing of nanoparticles. The tests could show the overall pattern of deterioration and guide the long-term performance of materials in outdoor conditions and help assess whether aging releases embedded fillers. To the best of our knowledge, only a limited amount of work has been done to systematically explore the effect of environmental aging on the thermal properties of MWCNT-polymer composites [15,16]. A multi-laboratory aging study of polyamide and epoxy-MWCNT composites done with standardized weathering equipment showed the release of MWCNTs [17]. However, extended UV-irradiation of epoxy-MWCNT-amine composite showed no detectable release of MWCNTs [18].

This paper is intended to initiate systematic kinetic studies of the aging of polymer nanocomposites in the understanding of the thermal behavior of these exciting materials since polymer structure changes during environmental weathering. The results of a rigorous investigation of the environmental effects on the thermal property changes of PP and PP-MWCNT having different thicknesses are report. The effects of environmental aging on thermal decomposition temperature, estimated degradation kinetics parameter, and activation energy, were investigated in detail. Analytical methods, such as differential scanning calorimetry (DSC) tests, were used to examine the changes in other thermal behaviors including melting and crystallization temperatures during the aging process [19–21].

2. Experimental

2.1 Preparation of polymer and polymer-nanocomposite test panels

PP (Isotactic, average MW ~250,000 and average MN ~67,000) was obtained from Sigma-Aldrich. Commercial MWCNTs (NANO-CYLTM NC7000, average diameter: 9.5 nm; average length: 1.5 mm, Batch number A2133) were obtained from the Nanocyl SA (Figs. S1(a) and (b)). The diameter of the MWCNTs was 10.9 ± 3.7 nm which is based on the

measurement of 9 individual MWCNT diameters using a transmission electron microscope (FEI TECNAI F20) (Fig. S1(b)).

Granular PP was mixed with 4% (w/w) MWCNTs in a heating chamber installed with mechanical mixing rods (Haake Rheocord 90, Thermo Electron Corporation, Waltham, MA). The selection of the weight content of MWCNTs (4 wt%) was based on the results of previous studies which reported a significant improvement of physicochemical and electrical properties of pristine materials using a weight fraction of nanofillers less than 5 wt% in different composites [22–24]. The mixing vessel temperature was maintained above the melting temperature ™ of PP (165 C) while it underwent high shear mixing for 30e60 min to achieve a uniform distribution of MWCNTs in PP. Afterward, the mixed materials were transferred to an extruder (Rheomex 102, USA) which was used to prepare test panels of PP and PP-MWCNT composites having three distinct thicknesses. The prepared test panels were denoted based on the composition of MWCNTs and thickness (Table 1). The thickness of the test panels was measured at least 3 times using a Vernier caliper and averaged. Scheme 1 (Supplementary Section) shows simplified procedures for the test panel preparation of PP and PP-MWCNT composite. As illustrated in Fig. 1, MWCNTs were well represented in the PP-MWCNT nanocomposite. The test panels were used for all aging experiments to evaluate changes in the thermal stability and other properties which occurred during or at the end of the aging process.

2.2 Aging of PP and PP-MWCNT nanocomposite

The effects of weather on the properties of PP and PP-MWCNT were studied using an accelerated environmental aging chamber (Suntest XLS, Atlas Material Testing Technology LLC). Test panels which were 5 cm by 5 cm and different thicknesses were held by screws onto a stainless steel mesh and placed in the aging chamber (Fig. S2). The test method used for this study adhered to the ISO- 4892-2/2013 method for accelerated aging which calls for 2 h sun and rain cycles [17,25]. The detailed experimental conditions for the weathering are provided in Table 2.

A cycle of weathering was repeated during the duration of the experiment (total 3024 h (18 weeks)). Samples of the PP and PP-MWCNT composites were collected at 0, 756, 1512, 2268, and 3024 h. The total amount of solar irradiation for each sampling time was recorded and converted to an approximate exposure time using annual solar radiant exposure data for subtropical regions (i.e., Florida, USA (6588 MJ/m^2)) [26]. A summary of the converted real exposure times during the aging experiment is provided in Table 3.

2.3 Characterizing environmentally aged PP-MWCNT composites

Differential scanning calorimetry (DSC) is a thermal analysis technique used to study thermal behaviors of materials, such as melting and crystallization temperatures, and the enthalpy of melting and crystallization. DSC was used for detecting the chemical and morphological changes that accompanied aging and degradation. Three to 4 mg of the composites were placed in an aluminum pan and subjected to controlled temperature variation. The sample pans and an empty reference pan were positioned in the DSC4 sample pan (TA, DSC Q2000, New Castle, DA) and heated simultaneously at a rate of 10 C/min

until a temperature of 200 C was reached. The temperature of each of the two pans was monitored, and the rate of heat flowing to the samples was adjusted to maintain the two samples at the same temperature. The T_m and crystallization (T_c) temperatures of PP and PP-MWCNT composite before and after aging were measured. The average of the replicate runs for each sample was used to calculate the heat flow at a given temperature (standard deviation 0.6 mcal/s/g).

Thermogravimetric analysis (TGA) technique measures the temperature dependence of the weight loss of samples due to thermal oxidation and the formation of volatile products. TGA (Pyrus 7, Perkin Elmer Inc.) was used to investigate changes in thermal stability due to the MWCNT reinforcement of PP, environmental aging, and test panel thickness. Over 100 surface samples of PP and PP-MWCNT (3.09 ± 0.14 mg) were taken following a similar protocol to minimize the variation in the analysis. The rate of the thermal decomposition depends on the temperature of the composite and the rate of heating, or the time that the sample is held at a given temperature. Therefore, the thermal decomposition kinetics of the TGA data provide parameters such as the activation energy, E_a, and the reaction order (k) [27]. The analytical conditions for TGA and DSC are summarized in Table 4.

The optical microscopy was carried out on aged composite surfaces using a digital microscope (HiRox Model KH 7700). A scanning electron microscope (JSM-6490LV, JEOL) was used to observe the MWCNTs that were used to prepare PP-MWCNT composites. A transmission electron microscope (TEM, JEM 2100, JEOL) was used to study the morphology of the PP-MWCNT composites.

2.4. Theoretical analysis

2.4.1. Crystallization—DSC studies are used to estimate the total crystalline content of polymers and composites based on the heat required to melt the polymer. An understanding of the degree of crystallinity of nanocomposite polymers as they age is important because crystallinity affects physical properties such as permeability, density, and melting point. For pristine and carbon nanotube reinforced polymers, the degree of crystallization, χ, can be quantified by measuring the heat associated with melting (fusion) of the polymer:

$$\chi = \frac{\Delta H_a}{\Delta H_m(1 - W_f)} \tag{1}$$

where ΔH_a is the measured enthalpies of melting which are obtained from the experiment by integrating the calorimetric signal, W_f is the weight fraction of the MWCNT content, and ΔH_m is the enthalpy fusion of a perfect crystal of 100% PP (207 J/g), having an infinite size [28–30].

2.4.2. Thermal decomposition iso-conversional kinetic method—Mass loss data from the thermogravimetric analysis can be used to calculate the conversion, which is the actual mass of sample decomposed. It can be defined as:

$$\alpha = \frac{m_o - m_t}{m_o} \tag{2}$$

where m_o is the initial mass of the sample and m_t is the sample mass at time t.

For the kinetics of the thermal decomposition of MWCNT using TGA, it can be assumed that the rate of decomposition is a function of both temperature and conversion:

$$\frac{\mathrm{d}\alpha}{\mathrm{dt}} = k(T)g(\alpha) \tag{3}$$

The temperature dependent function $k(T)$ in Eq. (3) is the specific rate constant commonly denoted by the Arrhenius equation:

$$k = Ae^{(-E/RT)} \tag{4}$$

is assumed for the temperature dependence of k, where A is the "pre-exponential factor," (1/min), is assumed to be independent of temperature, E is the energy of activation (J/mol) and R is the gas constant (8.314 J/mol K).

The conversion function is usually expressed as:

$$g(\alpha) = (\mathrm{n}-1)(1-\alpha)^{\mathrm{n}} \tag{5}$$

where n is the order of the reaction.

The decomposition kinetics equation is obtained by combining Equations (3)-(5):

$$\frac{\mathrm{d}\alpha}{\mathrm{dt}} = Aexp\left(\frac{-E(\alpha)}{RT}\right)(1-\alpha)^{n} \tag{6}$$

The actual temperature under non-isothermal temperature ramping conditions can be expressed using the following equation:

$$\mathrm{T} = \mathrm{T}_0 + \beta\mathrm{t} \tag{7}$$

where β is the heating rate (K/min) and T_0 is the initial temperature (K). From Equations (6) and (7), it can be shown that:

$$\frac{\mathrm{d}\alpha}{\mathrm{dt}} = \frac{A}{\beta}exp\left(\frac{-E(\alpha)}{RT}\right)(1-\alpha)^{n} \tag{8}$$

The integrated expression of Eq. (8) is:

$$\mathrm{F}(\alpha) = \int_0^{\alpha}\frac{\mathrm{d}\alpha}{(1-\alpha)^{n}} = \frac{A}{\beta}\int_{T_0}^{T}\left(\frac{-E(\alpha)}{RT}\right)\mathrm{dT} \tag{9}$$

Using Doyle's approximation method [31,32] after integrating Equation (9) and using logarithms, the result can be expressed as:

$$ln\beta = Constant - 1.052\left(\frac{E(\alpha)}{RT}\right) \quad (10)$$

The apparent activation energy, E, can be estimated based on a slope of a linear plot of lnβ versus $1/T$ to obtain the activation energy as a function of conversion, α [32]. Although the expressions used to evaluate these parameters are valid for fluid systems, but not for solid-state reactions, they are useful in the elucidation of mechanisms involved in polymer degradation.

3. Results and discussion

3.1. Characterization of pristine PP and PP-MWCNT nanocomposites with TGA and DSC

Non-isothermal TAG and DSC behaviors of PP and PP-MWCNT composites were studied. TGA and DTG curves for a heating rate of 10 °C/min showed single-stage high-temperature degradation with the onset decomposition temperature, $T_{onset,}$ around 400 °C with the maximum weight loss, $T_{peak,}$ at 470 ± 2.6 °C and 480 ± 3.2 °C for PP and PP-MWCNT composites, respectively (Fig. 2(a) and (b)). The reason for increased thermal stability could be that the dispersed nanotubes hindered the flux of the degradation products, which delayed the onset of degradation or the interaction between MWCNT and the macromolecular chains of PP slowed the degradation and shifted the T_{peak} [33].

The small variations in the percent weight loss of PP composites could be attributed to the manufacturing difference in crystal formation changes according to the heat treatment temperatures and cooling densities of thick test panels in using single screw PP sheet extrusion. The 50% weight loss temperature (T_{50}) for pure PP test panels decreased slightly as the panel thickness increased (Fig. 2(a)). PP has a density ranging from 0.855 g/cm^3 for the amorphous form to 0.946 g/cm^3 for the full crystalline form, and a melting temperature ranging from 130 °C to 170 °C. The decrease in T_{50} for the test panels of different thicknesses could be the result of the slight differences in crystallinity or the density of thicker samples. The rapid cooling is a potential source of error in the measured values when crystallized from the melt state in the skin of the injection mole. During the panel preparation, the lower pressure may apply to thicker test panels as test panels came out from the extruder. Thicker test panels may have low density compared to thin test panels due to micron size air pockets. It suggests that the added MWCNTs interacted with polypropylene, resulting in slightly improved thermal stability due to high mechanical and thermal stability of MWCNTs [7,8,34].

The melting point of PP and PP-MWCNT composites were 163 ± 0.6 °C and 162 ± 0.6 °C, respectively, which shows no significant difference, indicating there is no important interaction between MWCNTs and PP in the polymer matrix. The recrystallization temperature for MWCNTs-filled PP increased (Fig. 2(c) and (d)), which suggests that the added MWCNTs behave like nucleating agents for PP recrystallization [7]. This result differs from previous studies on the effects of a single-walled carbon nanotube on non-isothermal crystallization of PP, for which there was no significant change [35]. The increased recrystallization temperature of the PP-MWCNT composite may have restricted

sites for the PP segment, thereby inhibiting the formation of highly ordered spherulites and affecting the mechanism of nucleation and crystal growth [7,34]. The narrow, symmetrical and uniform crystallization curves suggest that heterogeneous nucleation is the predominant crystallization mechanism.

3.2. Weathering stress cracking of MWCT-PP composite

Semi-crystalline polymers, like PP, are essentially two phases systems containing spherulitic clusters of crystals surrounded by a continuum of amorphous substance. During the process of aging, PP and PP-MWCNT composites lost their elasticity and became brittle. Many cracks were formed on the surface of the composites. The light-water spray cycle resulted in photooxidation and hydrolysis which caused environmental stress cracking. Oxygen diffuses readily through the amorphous region, but diffusion through the crystalline regions is limited. As a result, most of the aging occurs at the spherulite boundaries and weakens the “glue” that holds the crystalline regions together. Fig. 3 shows SEM and optical microscopic images of pristine and aged PP test panels of increasing thicknesses (PP01, PP02 and PP03). The time it took for cracking and crumbling to occur was inversely proportional to the composite thickness, such that PP01 > PP02 > PP03. Craze formed as part of the crack initiation. The formation and growth of the cracks continued as aging progressed and the PP test panels also became increasingly brittle.

Although the PP-MWCNT composites demonstrated a higher resistance than pristine PP to aging cracks, the increased exposure resulted in significant changes in the surface structures (Fig. 4(a)-(d)). Aged composites showed evidence of exfoliation, surface holes and cracks. The depth of the surface cracks for composite PP42 increased from 50 μm to more than 80 μm as the aging time increased from 756 h to 2268 h, respectively (Fig. 4(c) and (d) inserts). The thickness of the oxidized layer can be determined from the depth of the cracked composites (Fig. 4(c) and (d)), which is related to the UV-aging time or dose.

Aging changes the structure of PP at the macromolecular, molecular, and the morphological levels and also induces variations in the chemical and structural properties. The exposed surfaces manifested crack propagation that increased over time and penetrated the layer close to the surface.

The diffusion of oxygen is significant for an accelerated test, especially in rapidly oxidizing polymers. Like most semi-crystalline polymers, PP oxidizes exclusively in the amorphous phase because the crystalline phase is impermeable to oxygen. Due to the presence of a methyl group in the tertiary carbon atom of the PP monomer backbone, the formation of unstable secondary free radicals is possible under oxidative conditions. This reaction is kinetically controlled by the diffusion of oxygen and water in the polymer. Therefore, the degraded layer of the PP is on the order of the ratio of the diffusion coefficient and the pseudo-first order kinetic coefficient of the rate constant, D/k [36–38].

3.3. Effect of aging on thermal stability of PP and PP-MWCNT composites

Aging and the presence of tertiary carbon in the chemical structure of PP causes degradation and changes in the chemical properties which are typically chain scission and crosslinking [39–42]. TGA measurements of polymers provide information on the thermal stability,

composition, decomposition profiles and formation of byproducts. The thermal stabilities of pristine and MWCNT-filled PP of three different thicknesses were investigated by TGA measurement both before and after environmental aging. The pyrolysis kinetics were based on weight loss versus temperature. Composites were heated at a rate of 10 °C /min. Thermogravimetric curves for pristine PP of selected thickness, PP01, PP02, PP03 and PP-MWCNT composites, PP41, PP42, and PP43 are shown in Fig. 5(a) and (f). PP degrades by a single mechanism for all pristine and aged composites, which suggests that it involves a similar rate-controlling step. However, the TGA curves indicate that the aged PP-MWCNT composites exhibit a significant reduction in thermal stability as the exposure time increased. As the duration of weathering increased to 3024 hr PP panels, the thinnest test panels, PP01, were found crumbled after 1512 h of aging, which was equivalent to an outdoor exposure of 6.9 months in Florida, U.S.A. and displayed a significant reduction in the T_{50} value from 470 °C to 434 °C (Fig. 5(a)). The PP thermal stability is affected by factors such as the presence of additive substances, changes in crosslinking due to aging, and the presence of aromatic rings and decomposing functional groups.

DTG data for the composites show a decrease in T_{peak} as the aging time increased (Supplemental Fig. S3). PP01 test panels completely broke into smaller pieces after 1512 h. PP02 test panels, which had a thickness of 0.39 ± 0.02 mm, fragmented after 2268 h. PP03 (0.69 ± 0.04 mm), by contrast, remained intact throughout the remainder of the test period, or 3024 h. Surface crack formations were associated with the contraction of the surface layer and the formation of chemi-crystallization [43]. As the intensity of cracking increased the materials became more fragile. The results showed that the effects of photooxidation originated on the exposed surface then diffused into the inner matrix. Therefore, the strength of the composite depended on the thickness of the composite.

TGA studies were conducted to monitor the decrease in T_{50} of PP-MWCNT composite specimens after weathering for selected periods of time. TGA curves for both pristine and PP-MWCNT composites exhibited a one-step decomposition, although the DTG curves for aged composites increased in width as the aging time increased. The TGA data for the three composites of increasing thicknesses, initial, and aged PP-MWCNT composites are shown in Fig. 5(d)-(f). The thicker PP-MWCNT composites demonstrated the highest thermal stability with a T50 value of 464 °C after 3024 h of weathering. Previous studies have reported that the thermal stability of aged polymer composites decreases because of the combined effects of photolysis, photooxidation, and the thermal degradation of composites [44–46]. Also, due to the MWCNT reinforcement, all PP-MWCNT composites displayed small amounts of structural break down during and after the weathering of 3024 h, which is the equivalent of 13.9 months of outdoor weathering.

TGA data show a slight drop in the weight of composites at temperatures less than 250 °C. For aged PP test panels, this may account for the loss of absorbed water, which promotes further degradation and impacts dimensional stability (Fig. 5(a)-(c)). Previous studies have revealed that absorbed water may exist in a polymer as free water or loosely bound water. Bound water can easily escape from the polymer during heating. Tightly bound water, which is strongly confined in the polymer network, requires additional energy to be removed from the polymer [47]. PP-MWCNT composites showed little or no absorption of moisture, even

after 3024 h of aging. The decomposition of PP due to weathering was caused by thermal, oxidative and hydrolytic reactions.

3.4. Environmental aging and changes in melting point

DSC can be used to analyze thermal effects and monitor the effects of environmental aging on various phenomena, including melting, crystallization, polymorphism, or specific heat. DSC analysis was used to monitor changes in the melting and crystallization temperatures of PP and PP-MWCNT composites that were being kept in the accelerated weathering chamber for selected periods of time. The data presented in Figs. 6 and 7 show changes in the melting and crystallization temperatures of pristine PP and PP-MWCNT composites before and after aging, respectively. The critical phase change data are summarized in Table 5.

The melting point depression of PP and PP-MWCNT was the result of aging to molecular chain scission and formation of carbonyl and hydroperoxide groups. The results of DSC analysis in Fig. 6(a),(c), and (e) show a T_m depression from 162.9 to 142.5 °C for PP01 after 1512 h of accelerated aging, and from 163.8 to 140.0 °C for PP02 after 2268 h. The T_m for PP03 dropped from 164.1 to 144.3 °C after 3024 h. Due to structural changes of aged composites by chain scission and oxidation, more aged composites began to melt at a lower temperature, which resulted in widening the range of melting temperatures. Similarly, there was a decrease in the melting temperature and extended temperature ranges of melting for aged PP-MWCNT composites (Fig. 7(a),(c), and (e)). However, the changes in the melting temperatures were not as significant as those associated with pristine PP. The measured T_m values for all pristine materials and after different environmental aging times are shown in Fig. 8(a). The changes in the T_m and T_c reflected the reduction in molecular weight and changes in the degree of crystallinity of the polymer matrix, which is caused by photolysis, photooxidation, and thermal degradation during weathering. These effects are more significant for thin composites of pristine PP than for PP-MWCNT. Fig. 7(b),(d) and (e) show smaller changes in the melting and crystallization temperature of PP-MWCNT composites than for aged-pristine PP. All composites show a broadening of melting that increased with aging. The largest observed change was 12.1 °C for PP41 and the smallest observed change was 2.4 °C for PP43. The melting temperature of PP01 decreased by more than 20 °C after 1512 h of aging. These results indicate that the added MWCNTs significantly increase the thermal stability of PP. The difference between both the melting and crystallization temperature before and after weathering of PP-MWCNT composites diminished with the increase in test panel thickness. The T_m and T_c of all aged PP-MWCNTs were higher than those for the aged pristine PP indicating that MWCNTs significantly improved the thermal stability of PP.

Brzozowska-stanuch et al. [44] studied thermal property changes of PP containing different materials (i.e., montmorillonite, compatibilizer, MWCNTs, and blue pigment) by UV aging following the standard method by Society of Automotive Engineers (SAE J2527). They reported that the melting and crystallization temperature of aged PP composites decreased due to structural changes such as polymer chains shortening in the aged composites. However, they also reported there were minimal changes in the thermal stability of composites containing MWCNTs by UV [44]. The decrease of T_m and T_c lessened when as

the thickness of the composites increased. This signifies that the decomposition of polymers by weathering started on the surface of polymers. Specifically, that changes in both the melting and crystallization temperature of the PP43 composite are small - only 2 °C decrease - implying that MWCNTs reinforced the thermal properties of PP and that polymer decomposition by weathering occurs at the polymer surface, followed by gradual degradation inside of the polymers [47,48].

3.5. Environmental aging and recrystallization

The estimated degree of crystallinity of aged composites increased as the result of weathering (Fig. 8(d)). The thicker composites crystallized slower than the thinner composites. Previous studies [49–51] also reported results that showed an increase in crystallinity of the polymer composites after aging, which could be attributed to the reduction of the amorphous fraction and the rearrangement of crystals induced by chain scission and changes in molecular size during the aging process. However, due to the complexity of changes in the structural and chemical properties of polymers during the aging process, the crystallinity may increase or decrease [52].

In addition to investigating the thermal properties of aged PP and PP-MWCNT composites, a DSC analysis was performed to evaluate the aging of the polymer along its depth from the surface exposed to direct irradiation. The thickest composite, PP43, was chosen because three different parts (i.e., top (exposed surface toward solar light), middle (inside), and bottom (unexposed surface)) could be taken from this composite only due to its thickness of approximately 2 mm. As shown in Fig. S5(a), the melting temperature of different parts varied by 2 °C at time 0. The degree of crystallinity of each part was approximately 4.6% for the top part, 6.0% for the middle part, and 3.7% for the bottom part. As the aging advanced, the degree of crystallinity of the top and bottom parts of PP gradually increased. Composites were taken from the surface of irradiated panels at selected aging times exhibited increasing degree of crystallinity. The changes in crystallinity were less significant for the unexposed side of the panel (Fig. S5(b)). The changes in crystallinity imply that photolysis and photooxidation occur mainly at the surface of the composites that are exposed to solar light, and the accumulated heat triggers the thermal degradation of composites from the surface to the inside, resulting in the decomposition of the inside of composites by a long-term aging process.

The DSC data on the effects of aging on the melting and recrystallization temperatures of PP and PP-MWCNT composites are summarized in Fig. 8(a)-(b). The melting temperature depression was measured, and the rate was determined to be ~1 °C for every 75 h (for PP01) to 110 h (for PP03) of exposure, depending on the panel thickness. For PP-MWCNT, a decrease of 1 °C in the melting point was measured ranging from every 150 °C for the thin test panels (PP41) to every 320 °C for PP43 (Fig. 8(a)). DSC measures indicate that the recrystallization temperatures were more than 10 °C higher for the PP-MWCNT composites and that they were not affected by aging, although the degree of crystallinity increased (Fig. 8(b) and (d)). The decrease of polymer stability, as shown, is based on a comparison of the decline of T_{50} with aging time, which indicates changes in the polymer molecular structures

(Fig. 8(c)). The slope of the decline depends on the thickness of the composite and composition that shows the photooxidation of polymers is primarily a surface phenomenon.

3.6. Fourier-transfer infrared spectroscopy

Fig. 9(a)-(d) show recorded FT-IR spectra of the surfaces of pristine and aged samples of PP and PP-MWCNT composite. For all pristine samples of PP and PP-MWCNT composites the characteristic peaks of alkyl C-H stretch from 2970 cm^{-1} cm^{-1} to 2840 cm^{-1} cm^{-1} were observed Fig. 9(a) and (b). The two peaks at 1460 cm-1 and 1370 cm-1, corresponding to the bending of functional groups -CH2- and -CH3, respectively. These results are in good agreement with the previous FT-IR studies of environmental degradation of polypropylene [53–55]. There were no differences in FT-IR spectra between pristine PP and PP-MWCNT composites. It may be because of functionalized MWCNTs embedded in the polymer were pure carbon. After aging the PP test panels for selected times of 1512 h, 2268 h and 3024 h, for samples PP01, PP02 and PP03, the peak height of the FTIR spectra decreased from 2970 cm^{-1} to 2840 cm^{-1} (Fig. 9(c) and (d)), These decrease indicate the degradation of polypropylene due to molecular chain scission by weathering. The increase in spectrum peak height at 1850 cm^{-1} to 1540 cm^{-1}, corresponding to formation of carbonyl groups and carboxylate bands. The broad peak was observed from 3600 cm^{-1} to 3000 cm^{-1}, corresponding to hydrogen-oxygen bond [53–56]. These surface FTIR results indicate that the surface of aged composite surfaces was oxidized due to photooxidation during the weathering process. In particular, a broad peak from 2150 cm^{-1} to 2020 cm^{-1}, corresponding to carbonyls, in aged PP-MWCNT composites was observed [57] as seen in Fig. 9(d). It might be due to the oxidation of MWCNTs added in the polymer matrix during the weathering process.

3.7. Thermogravimetric analysis of aged polypropylene-MWCNT

This study estimated the change in one kinetic parameter, the activation energy, E_a, for pristine and aged PP and PP-MWCNT composites. E_a is the most important kinetic parameter, and it can be used to predict the material storage and operating life [58]. Isoconversional kinetics is an easy-to-use method for kinetics evaluation, and it is good for approximating complex experimental data. The rate of thermal degradation can be parameterized by the extent of conversion as a function of temperature. However, the method is not directly linked to particular species or reaction molecules of the aged composites. The method typically reflects the overall transformation of the various reactants to products during the TGA runs.

The calculated E_a, values ranged from 0.05 to 0.95 with a step of 0.05. The values of E_a were evaluated using the isoconversion method, which allowed for a mechanism and analysis of decomposition kinetics. A TGA analysis was conducted of all composites at the selected heating rates of 10, 20, 40, or 50 C min^{-1} in order to estimate the activation energies. The isoconversional lines for predefined conversion were calculated using the data collected for the different heating rates based on Equation (10), section 2.4.2. The linear plots of ln β versus 1/T taken from the aged composite panels with different conversion values, α. These values are used to estimate thermal decomposition kinetic parameter, E_a, from the slopes of the linear plots (Figs. S6-S11). The estimated effective E_a values are

shown in Fig. 10(a)e-(f). At $\alpha = 0.1$, the activation energies for pristine PP01, PP02, and PP03 were 338, 338, and 346 kJ/mol, respectively. PP-MWCNT composites had higher E_a, values of 380 kJ/mol, 280 kJ/mol and 350 kJ/mol for PP41, PP2, and PP43, respectively. This confirms the increase in thermal stability. It is evident the activation energies after aging decreased significantly with longer aging time. The activation energies for thermal decomposition for material loss from 10% to 50% conversion were significantly lower, which reveals that dominant kinetic process is changing. These results are similar to the values reported in the literature [59]. The activation energy of aged PP01, PP02 and PP03 at 50% conversion indicated significant reduction to 156 kJ/mol, 128 kJ/mol, 195 kJ/mol after exposure from 1500 to 3024 h. The decrease in the activation energy of aged PP-MWCNT composites was lower than pristine material but not as significant as unfilled PP. The value of E_a for the pristine PP and PP-MWCNT composite was nearly constant with thermal conversion, α. However, for the aged composites, the significant variation in E_a indicates the thermally stimulated decomposition processes are kinetically complex. The increased non-linear relationship of E_a with conversion as the PP and PP-MWCNT composites age indicted multistep decomposition kinetics. Weathering degrades the molecular structure of the amorphous fraction and disintegrated weak links that fragmented polymer chains and added carbonyls resulting in a decrease of the activation energy. However, varied patterns of the estimated activation energy over weathering times were observed for each composite due to the complexity of changes in structural and chemical properties during polymer degradation [52,60]. Moreover, the activation energy for thin composites rapidly decreased compared to thicker composites, indicating that polymer degradation started from the surface of composites and proceeded to the inner matrix of the composites.

4. Conclusions

The property changes of PP and PP-MWCNT nanocomposites during the environmental aging were investigated using thermal analysis techniques to discern the effects of composite thickness and the filling of MWCNT. Environmental aging of PP has a significant influence on changes in T_{50}, melting and crystallization temperatures, the degree of crystallinity, and the thermal decomposition kinetic parameter, E_a. TGA analysis showed that T_{50} values decreased significantly for the pristine PP when aged, and there was a direct correlation between the decrease in T_{50}, T_m, and T_c and the aging time. The thin PP panels crumbled during the test period, which confirmed that accelerated aging is controlled by surface reaction mechanism.

All tests that compared pristine PP with MWCNT-PP composites showed that the MWCNT loading increased the thermal stability of PP. Melting and crystallization temperatures decreased with prolonged weathering times while the degree of crystallinity increased for all aged composites.

There was a remarkable decrease in the melting and crystallization temperatures of aged PP panels. For PP01 test panels, a 20 °C drop in the melting temperature was measured after 1512 h of weathering while a reduction of 12 °C was measured for aged PP41 after 3024 h of aging. The increased stability is due to the presence of MWCNTs in the PP-MWCNT composites. For all composites, the decrease of the melting and crystallization temperatures

was inversely proportional to the thickness of composites during the aging process. The crystallinity of the composites was independent of the composite depths and increased by rearrangement of crystals induced by chain scission and changes of molecular size during the aging process. The activation energy, the kinetic parameters of polymer degradation, was estimated. At $\alpha = 0.1$, the activation energy of all composites decreased when exposed to solar light for longer periods of time, and the decrease was inversely proportional to the composite thicknesses. However, because of the complexity of changes in the structural and chemical properties of composites during weathering, different patterns of the activation energy were obtained for each composite by the estimation study.

The results of this study demonstrated changes in the thermal properties of PP and PP-MWCNT composites during accelerated weathering using thermogravimetric and calorimetric analyses. This indicates that these analytical techniques are useful for studying and understanding the degradation of polymers while aging in the environment, or when polymers are disposed of during, or at the end, of their use.

Supplementary Material

Refer to Web version on PubMed Central for supplementary material.

Disclaimer and Acknowledgement

The views expressed in this manuscript are those of the authors and do not necessarily represent the views or policies of the U.S. Environmental Protection Agency. This study was supported in part by appointment to the Internship/Research Participation Program at the National Risk Management Research Laboratory, U.S. Environmental Protection Agency, administered by the Oak Ridge Institute for Science and Education through an interagency agreement between the U.S. Department of Energy and EPA.

References

1. de Dicastillo CL, Castro-López M. del Mar, López-Vilariño JM, González-Rodríguez MV, Immobilization of green tea extract on polypropylene films to control the antixodiant activity in food packaging, Food Res. Int 53 (2013) 522–528.
2. Ellis TS, D'Angelo JS, Thermal and mechanical properties of a polypropylene nanocomposite, J. Appl. Polym. Sci 90 (6) (2003) 1639–1647.
3. Lepot N, Van Bael MK, Van den Rul H, D'Haen J, Peeters R, Rfanco J, Mullens D, Influence of incorporation of ZnO nanoparticles and biaxial orientation on mechanical and oxygen barrier properties of polypropylene films for food packaging applications, J. Appl. Polym. Sci 120 (2011) 1616–1623.
4. Vassiliou V, Bikiaris D, Chrissafis K, Paraskevopoulos KM, Staverv SY, Docoslis, Nanocomposites of isotactic polypropylene with carbon nano-particles exhibiting enhanced stiffness, thermal stability and gas barrier preterites, Compos. Sci. Technol 68 (3–4) (2008) 933–943.
5. Chen W, Tao X, Xue P, Cheng X, Enhanced mechanical properties and morphological characterizations of poly(vinyl alcohol)-carbon nanotube composite films, Appl. Surf. Sci 252 (2005) 1404–1409.
6. Kim JY, Han SI, Hong S, Effect of Modified carbon nanotube on the properties of aromatic polyester nanocomposites, Polymer 49 (15) (2008) 3335–3345.
7. Manchado ML, Valentini L, Biagiotti J, Kenny J, Thermal and mechanical properties of single-walled carbon nanotubes-polypropylene composites prepared by melt processing, Carbon 43 (7) (2005) 1499–1505.

8. Prashantha K, Soulestin J, Lacrampe M, Krawczak P, Dupin G, Claes M, Masterbatch-based multi-walled carbon nanotube filled polypropylene nanocomposites: assessment of rheological and mechanical properties, Compos. Sci. Technol 69 (11) (2009) 1756–1763.
9. Zeng H, Gao C, Wang Y, Watts PC, Kong H, Cui X, Yan D, In situ polymerization approach to multiwalled carbon nanotubes-reinforced nylon 1010 composites: mechanical properties and crystallization behavior, Polymer 47 (1) (2006) 113–122.
10. Du J, Wang S, You H, Zhao X, Understanding the toxicity of carbon nano-tubes in the environment is crucial to the control of nanomaterials in producing and processing and the assessment of health risk for human: a review, Environ. Toxicol. Pharmacol 36 (2) (2013) 451–462. [PubMed: 23770455]
11. Lam C.-w., James JT, McCluskey R, Arepalli S, Hunter RL, A review of carbon nanotube toxicity and assessment of potential occupational and environmental health risks, Crit. Rev. Toxicol 36 (3) (2006) 189–217. [PubMed: 16686422]
12. Liu Y, Zhao Y, Sun B, Chen C, Understanding the toxicity of carbon nano-tubes, Accounts Chem. Res 46 (3) (2012) 702–713.
13. Boddu V, Redner P, Energetic Materials: Thermophysical Properties, Predictions, and Experimental Measurements, CRC Press, 2010.
14. Sahle-Demessie E, Han C, Zhao A, Hahn B, Grecsek H, Interaction of engineered nanomaterials with hydrophobic organic pollutants, Nanotechnology 27 (28) (2016) 284003. [PubMed: 27265536]
15. Ghorbel I, Thominette F, Spiteri P, Verdu J, Hydrolytic aging of poly-carbonate. I. Physical aspects, J. Appl. Polym. Sci 55 (1) (1995) 163–171.
16. Raghavan D, Torma A, DSC and FTIR characterization of biodegradation of polyethylene, Polym. Eng. Sci 32 (6) (1992) 438–442.
17. Wohlleben W, Kingston C, Carter J, Sahle-Demessie E, Vázquez-Campos S, Acrey B, Chen C-Y, Walton E, Egenolf H, Müller P, NanoRelease: pilot interlaboratory comparison of a weathering protocol applied to resilient and labile polymers with and without embedded carbon nanotubes, Carbon 113 (2017) 346–360. [PubMed: 30147114]
18. Nguyen T, Petersen EJ, Pellegrin B, Gorham JM, Lam T, Zhao M, Sung L, Impact of UV irradiation on multiwall carbon nanotubes in nanocomposites: formation of entangled surface layer and mechanisms of release resistance, Carbon 116 (2017) 191–200. [PubMed: 28603293]
19. Corrales T, Catalina F, Peinado C, Allen N, Fontan E, Photooxidative and thermal degradation of polyethylenes: interrelationship by chemiluminescence, thermal gravimetric analysis and FTIR data, J. Photochem. Photobiol. A Chem 147 (3) (2002) 213–224.
20. Mandelkern L, Characterization of Crystalline Polymers by Raman Spectroscopy and Differential Scanning Calorimetry, Polymer Characterization: Physical Property, Spectroscopic, and Chromatographic Methods, 1988, pp. 377–395.
21. Porter CE, Blum FD, Thermal characterization of PMMA thin films using modulated differential scanning calorimetry, Macromolecules 33 (19) (2000) 7016–7020.
22. Gentile G, Ambrogi V, Cerruti P, Di Maio R, Nasti G, Carfagna C, Pros and cons of melt annealing on the properties of MWCNT/polypropylene composites, Polym. Degrad. Stab 110 (2014) 56–64.
23. Kashiwagi T, Grulke E, Hilding J, Groth K, Harris R, Butler K, Shields J, Kharchenko S, Douglas J, Thermal and flammability properties of poly-propylene/carbon nanotube nanocomposites, Polymer 45 (12) (2004) 4227–4239.
24. Winey KI, Vaia RA, Polymer nanocomposites, MRS Bull. 32 (04) (2007) 314–322.
25. Wohlleben W, Neubauer N, Quantitative rates of release from weathered nanocomposites are determined across 5 orders of magnitude by the matrix, modulated by the embedded nanomaterial, NanoImpact 1 (2016) 39–45.
26. AMETEK®, Benchmark Climates, http://atlas-mts.com/services/natural-weathering-testing-services/static-weathering/benchmark-climates/ (Retrieved February 23, 2017).
27. Flynn JH, Wall LA, A quick, direct method for the determination of activation energy from thermogravimetric data, J. Polym. Sci. Part C Polym. Lett 4 (5) (1966) 323–328.

28. Longo C, Savaris M, Zeni M, Brandalise RN, Grisa AMC, Degradation study of polypropylene (PP) and disoriented polypropylene (BOPP) in the environment, Mater. Res 14 (4) (2011) 442–448.
29. Mutlur S, Thermal Analysis of Composites Using DSC, Advanced Topics in Characterization of Composites, 2004, pp. 11–33.
30. Van der Wal A, Mulder J, Gaymans R, Fracture of polypropylene: the effect of crystallinity, Polymer 39 (22) (1998) 5477–5481.
31. Doyle C, Kinetic analysis of thermogravimetric data, J. Appl. Polym. Sci 5 (15) (1961) 285–292.
32. Vyazovkin S, Isoconversional Kinetics of Thermally Stimulated Processes, Springer, 2015.
33. Chipara M, Lozano K, Hernandez A, Chipara M, TGA analysis of poly-propyleneecarbon nanofibers composites, Polym. Degrad. Stab 93 (4) (2008) 871–876.
34. Assouline E, Lustiger A, Barber A, Cooper C, Klein E, Wachtel E, Wagner H, Nucleation ability of multiwall carbon nanotubes in polypropylene composites, J. Polym. Sci. Part B Polym. Phys 41 (5) (2003) 520–527.
35. Li L, Li B, Hood MA, Li CY, Carbon nanotube induced polymer crystallization: the formation of nanohybrid shish-kebabs, Polymer 50 (4) (2009) 953–965.
36. Audouin L, Langlois V, Verdu J, Bruijn J.d., Role of oxygen diffusion in polymer ageing: kinetic and mechanical aspects, J. Mater. Sci 29 (3) (1994) 569–583.
37. Kagiya T, Nishimoto S, Watanabe Y, Kato M, Importance of the amorphous fraction of polypropylene in the resistance to radiation-induced oxidative degradation, Polym. Degrad. Stab 12 (3) (1985) 261–275.
38. Zhang XC, Butler MF, Cameron RE, The relationships between morphology, irradiation and the ductile-brittle transition of isotactic polypropylene, Polym. Int 48 (11) (1999) 1173–1178.
39. Gugumus F, Effect of temperature on the lifetime of stabilized and unstabilized PP films, Polym. Degrad. Stab 63 (1) (1999) 41–52.
40. Gupta V, Drzal L, Rich M, The physical basis of moisture transport in a cured epoxy resin system, J. Appl. Polym. Sci 30 (11) (1985) 4467–4493.
41. Obadal M, Čermák R, Raab M, Verney V, Commereuc S, Fraïsse F, Structure evolution of a-and b-polypropylenes upon UV irradiation: a multiscale comparison, Polym. Degrad. Stab 88 (3) (2005) 532–539.
42. Rabello M, White J, The role of physical structure and morphology in the photodegradation behaviour of polypropylene, Polym. Degrad. Stab 56 (1) (1997) 55–73.
43. De Paoli MA, Degradação e estabilização de polímeros, Artliber São Paulo, 2009.
44. Brzozowska-Stanuch A, Rabiej S.a., Fabia J, Nowak J, Changes in thermal properties of isotactic polypropylene with different additives during aging process, Polimery 59 (4) (2014) 302–307.
45. Rabello M, White J, Crystallization and melting behaviour of photodegraded polypropylene-I. Chemi-crystallization, Polymer 38 (26) (1997) 6379–6387.
46. Wiles DM, Scott G, Polyolefins with controlled environmental degradability, Polym. Degrad. Stab 91 (7) (2006) 1581–1592.
47. Bumbudsanpharoke N, Ko S, A study of thermal properties of LDPE-nanoclay composite films, Korean J. Packag. Sci. Technol 21 (3) (2015) 107–113.
48. Pires HM, Mendes LC, Cestari SP, Pita VJRR, Effect of weathering and accelerated photoaging on PET/PC (80/20 wt/wt%) melt extruded blend, Mater. Res 18 (4) (2015) 763–768.
49. Bhateja S, Radiation-induced crystallinity changes in linear polyethylene: influence of aging, J. Appl. Polym. Sci 28 (2) (1983) 861–872.
50. Bhateja S, Andrews E, Yarbrough S, Radiation induced crystallinity changes in linear polyethylenes: long term aging effects, Polym. J 21 (9) (1989) 739–750.
51. Gal O, Kostoski D, Babi c D, Stannett V, DSC melting behavior of irradiated low density polyethylenes containing antioxidants, Int. J. Radiat. Appl. Instrum. Part C. Radiat. Phys. Chem 28 (3) (1986) 259–267.
52. Carrasco F, Pages P, Pascual S, Colom X, Artificial aging of high-density polyethylene by ultraviolet irradiation, Eur. Polym. J 37 (7) (2001) 1457–1464.

53. Barbes L, Radulescu C, Stihi C, ATR-FTIR spectrometry characterisation of polymeric materials, Rom. Rep. Phys 66 (3) (2014) 765–777.
54. Silva RA, Silva P, Carvalho M, Degradation Studies of Some Polymeric Bio-materials: Polypropylene (PP) and Polyvinylidene Difluoride (PVDF), Materials science forum, Trans Tech Publ, 2007, pp. 573–576.
55. Wen Z, Shen XH,D, The FTIR studies of photo-oxidative degradation of polypropylene, Chin. J. Polym. Sci 6 (3) (1988) 285–288.
56. Mylläri V, Ruoko TP, Syrjälä S, A comparison of rheology and FTIR in the study of polypropylene and polystyrene photodegradation, J. Appl. Polym. Sci 132 (28) (2015).
57. Kondarides DI, Chafik T, Verykios XE, Catalytic reduction of NO by CO over rhodium catalysts: 3. The role of surface isocyanate species, J. Catal 193 (2) (2000) 303–307.
58. Bystritskaya EV, Monakhova TV, Ivanov VB, TGA application for optimising the accelerated aging conditions and predictions of thermal aging of rubber, Polym. Test 32 (2) (2013) 197–201.
59. Peterson JD, Vyazovkin S, Wight CA, Kinetics of the thermal and thermo-oxidative degradation of polystyrene, polyethylene and poly (propylene), Macromol. Chem. Phys 202 (6) (2001) 775–784.
60. Chigwada G, Kandare E, Wang D, Majoni S, Mlambo D, Wilkie CA, Hossenlopp JM, Thermal stability and degradation kinetics of polystyrene/organically-modified montmorillonite nanocomposites, J. Nanosci. Nanotechnol 8 (4) (2008) 1927–1936. [PubMed: 18572595]

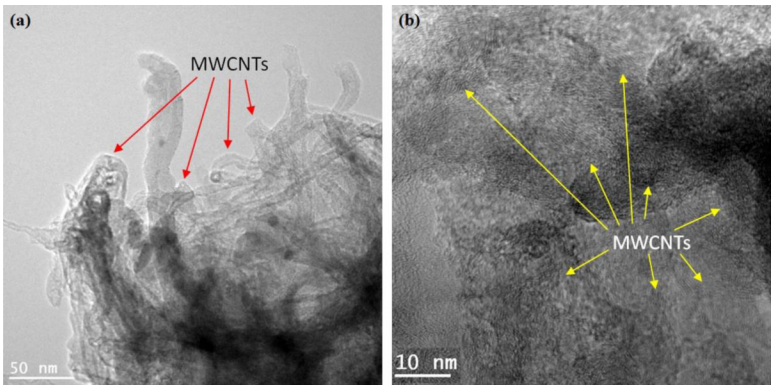

Fig. 1.

Transmission electron micrographs (TEM) of polypropylene-MWCNT composite (a) a sectioned panel, (b) lateral surface of composite panel.

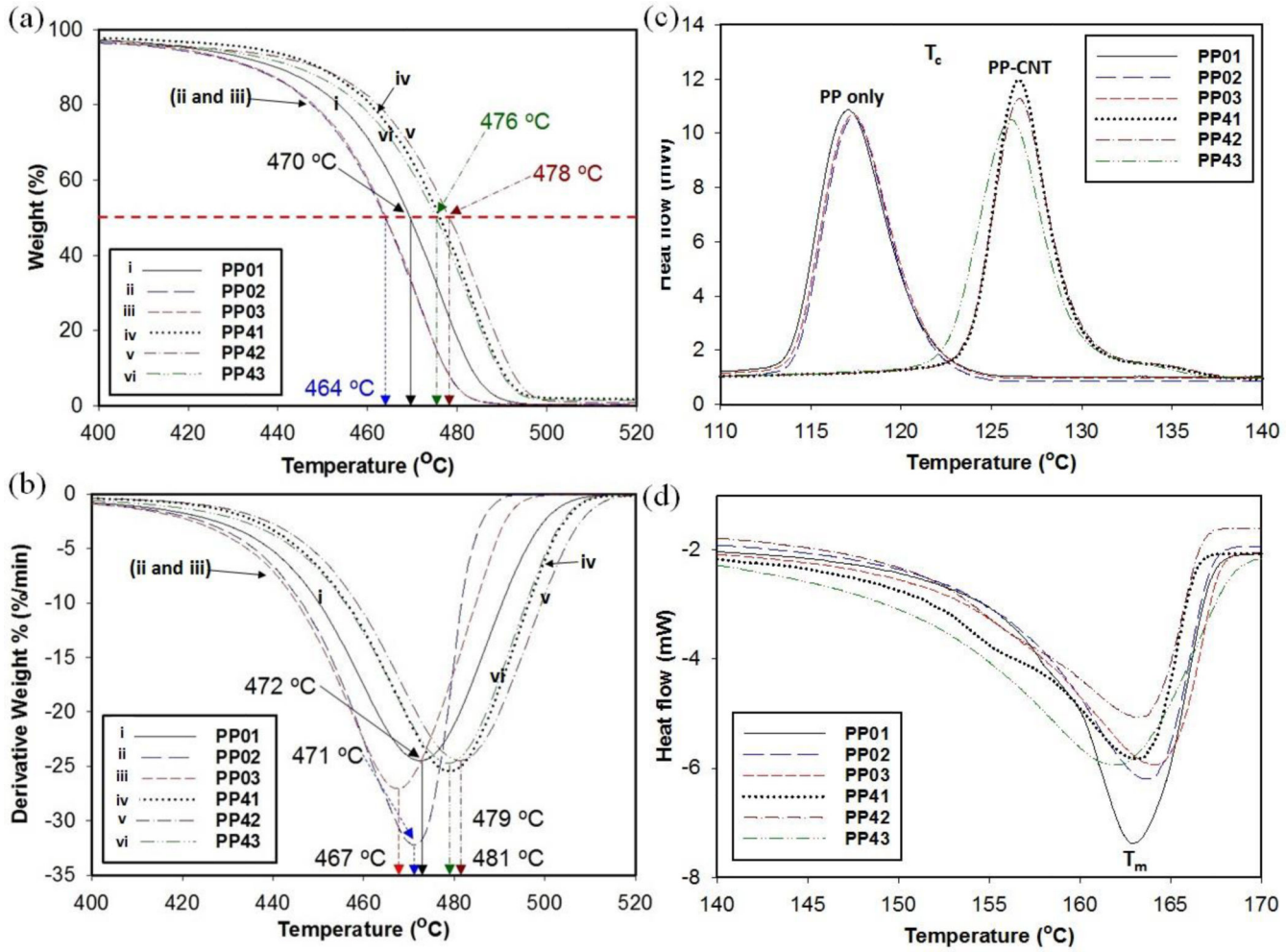

Fig. 2.

Thermal analysis of unfilled PP and PP-MWCNT composites samples of varying thickness (a) TGA curves (b) differential thermometric curves (DTA), (c) DSC curves of recrystallization temperatures, and (d) DSC of melting temperatures.

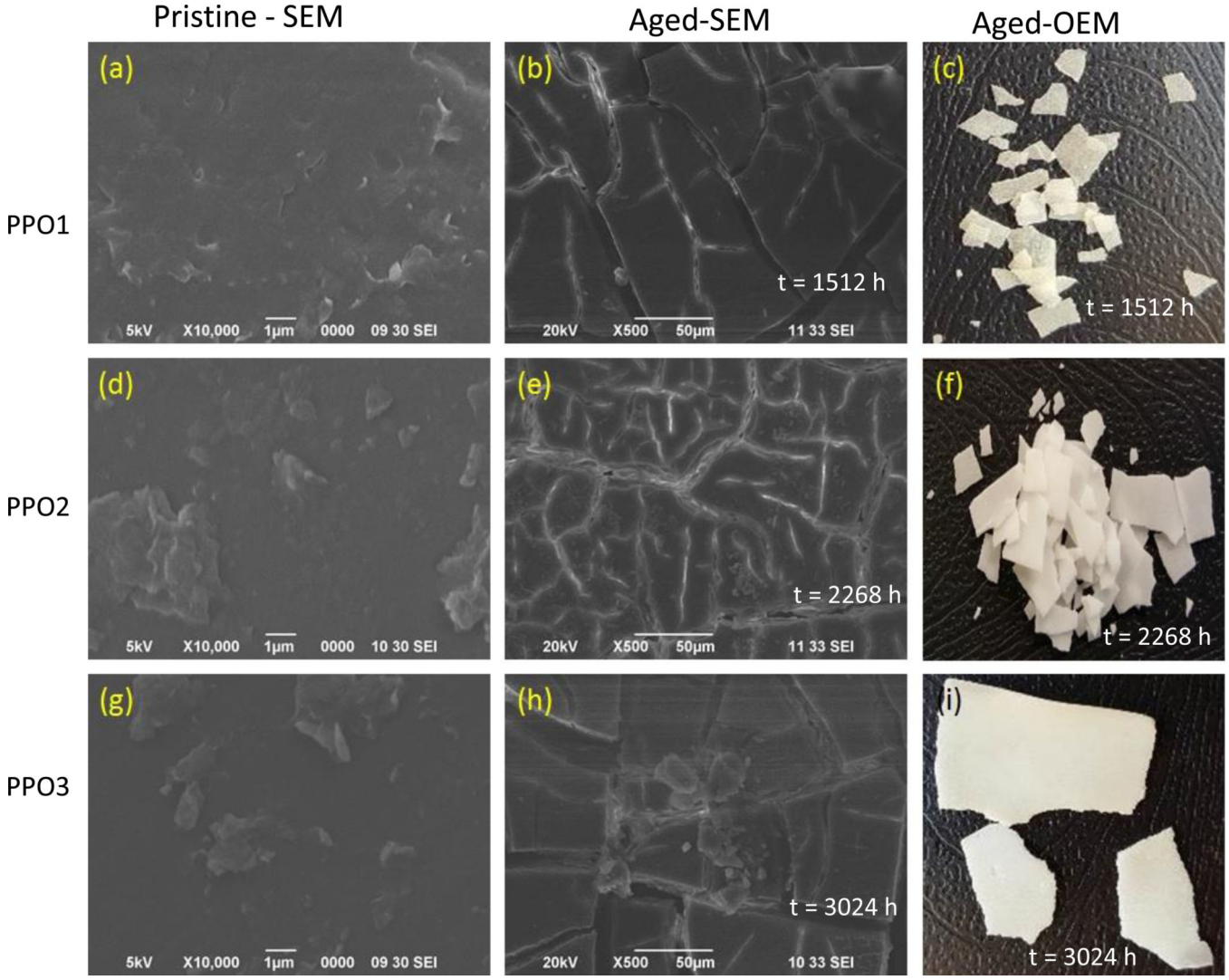

Fig. 3.

Representative scanning electron microscope (SEM) and optical microscope (OM) images of pristine and environmentally aged for selected times (a) to (c) for PP01, (d) to (f) for PP02, (g) to (i) for PP03.

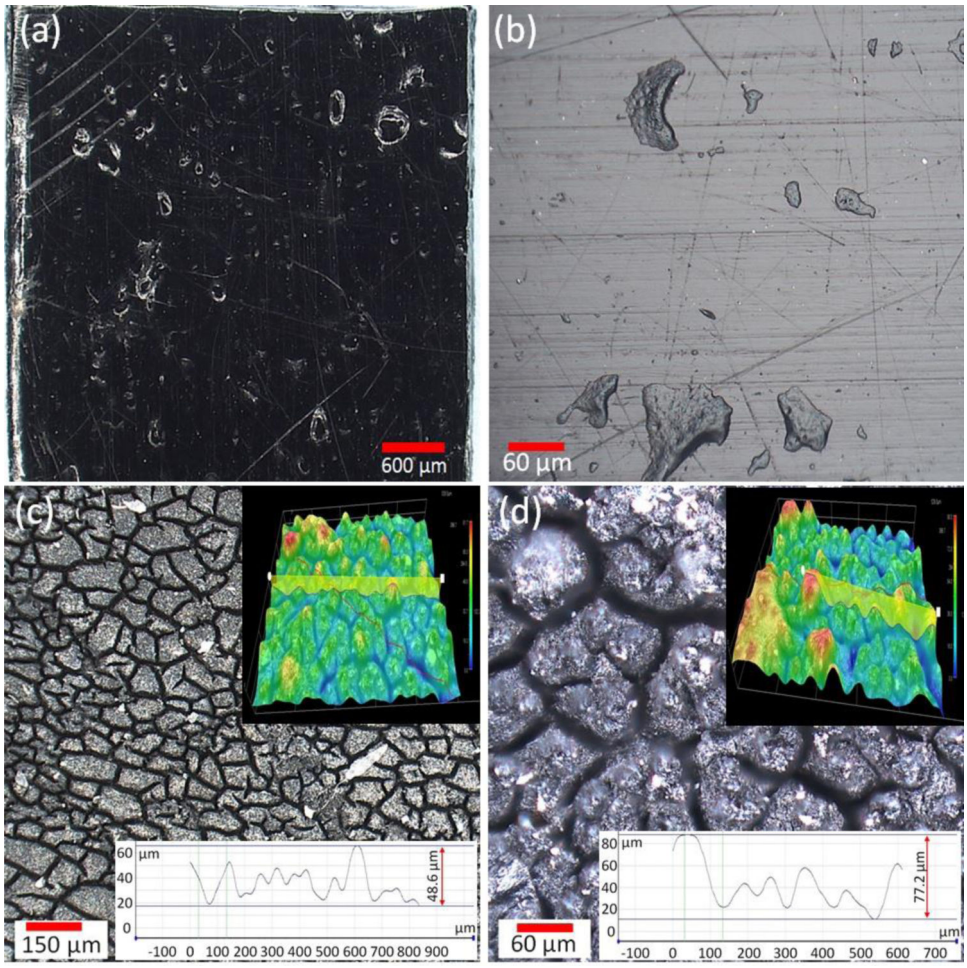

Fig. 4.

Representative optical images of PP-MWCNT composite samples (PP42) (a) and (b) pristine, (c) aged for 756 h, and (d) aged for 2268 h. Inserted images show 3D digital images of PP42 sample aged for 756 h and 2268 h, and) surface-valley crack profiles for PP42 samples.

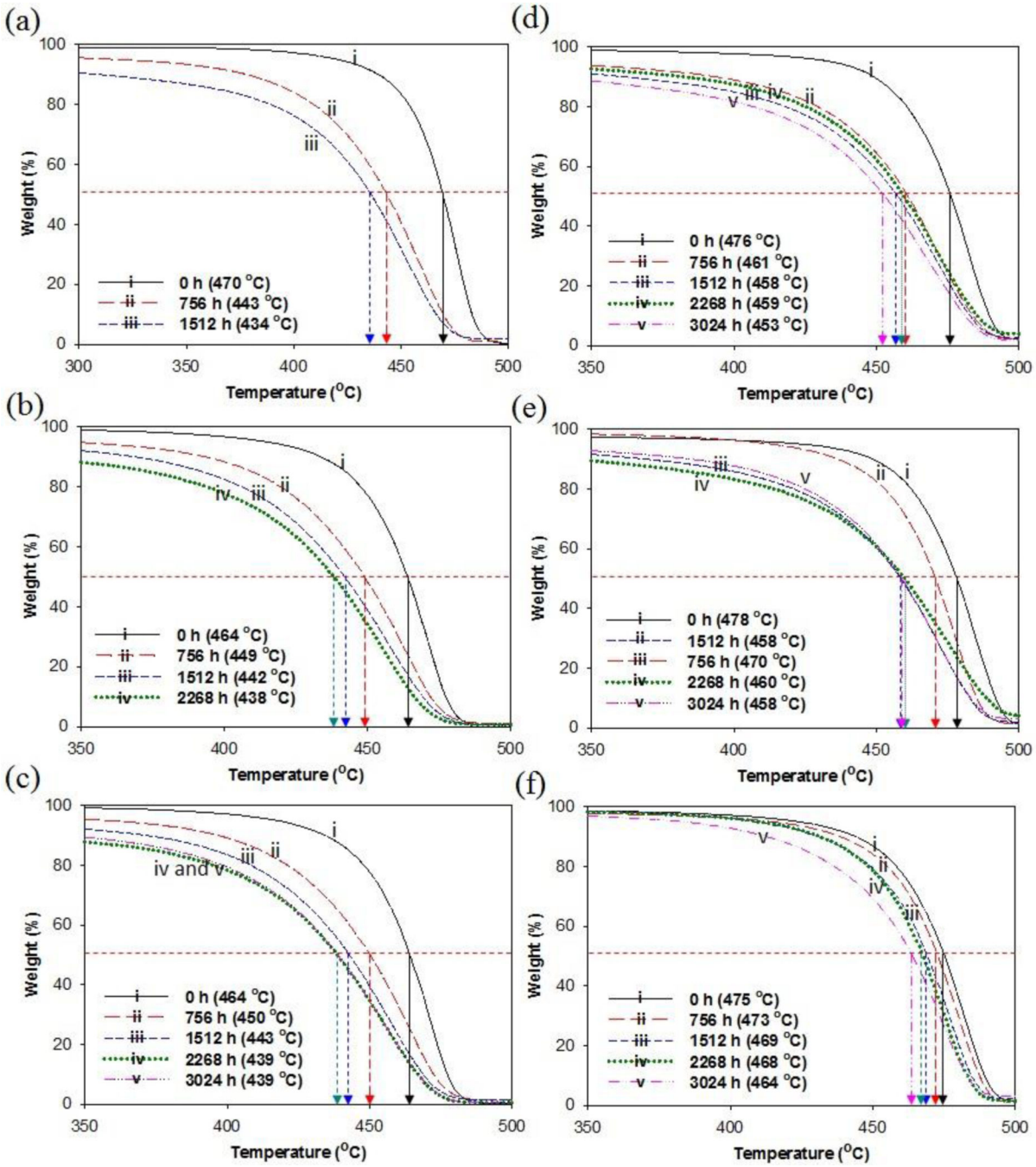

Fig. 5.

Thermograms of pristine and aged unfilled PP (a) PP01 (L = 0.25 mm), (b) PP02 (L = 0.39 mm), (c) PP03 (L = 0.69 mm), and PP-MWCNT composites (d) PP41 (L = 0.35 mm), (e) PP42 (L = 0.50 mm), and (f) PP43 (L = 2.27 mm) by accelerated weathering. (L = panel thickness).

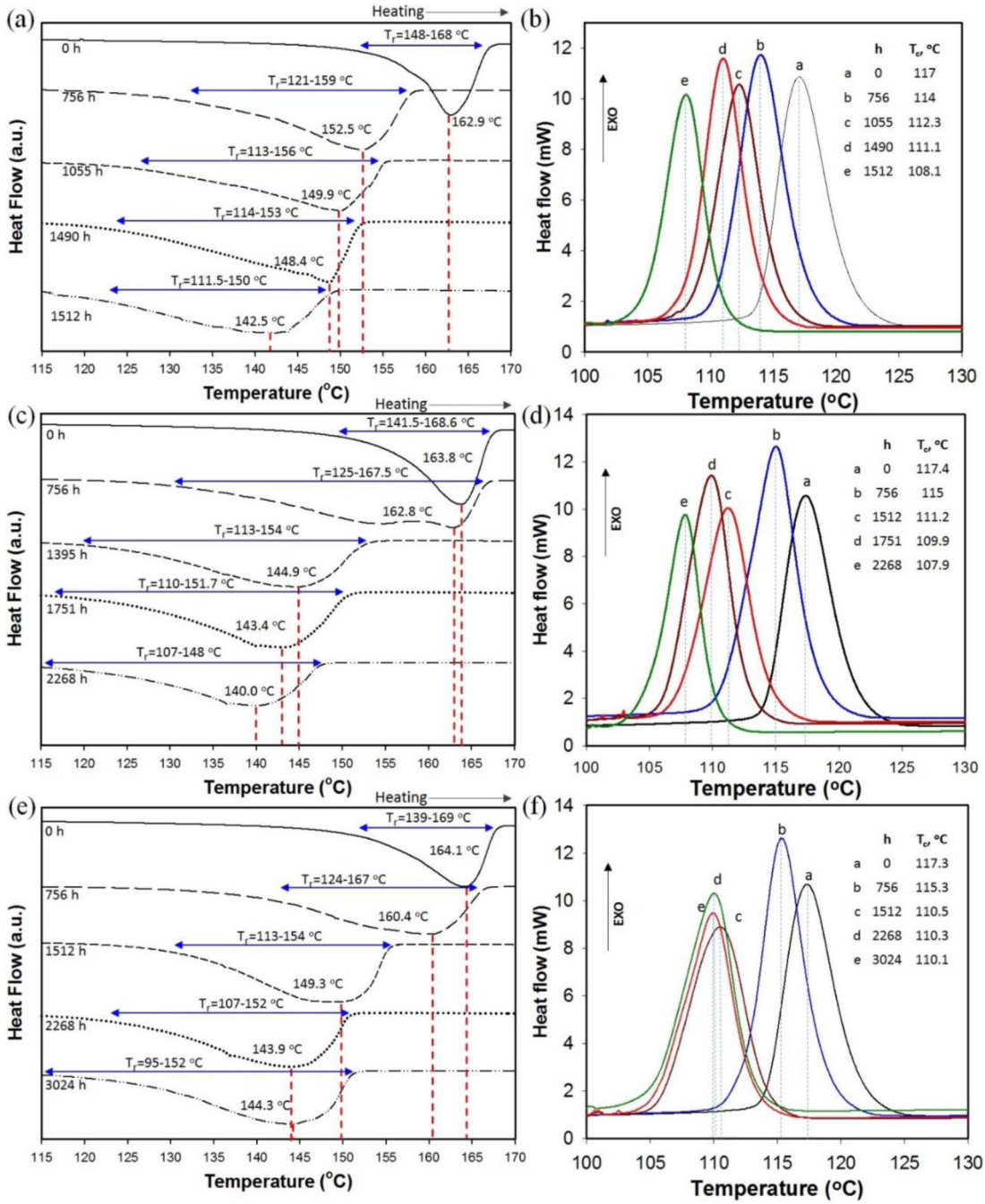

Fig. 6.

Representative DSC thermograms of unfilled PP for selected aging times showing (a) melting and (b) recrystallization temperatures for PP01, (c) melting and (d) recrystallization temperatures of PP02, and (e) melting and (f) recrystallization temperatures of PP03.

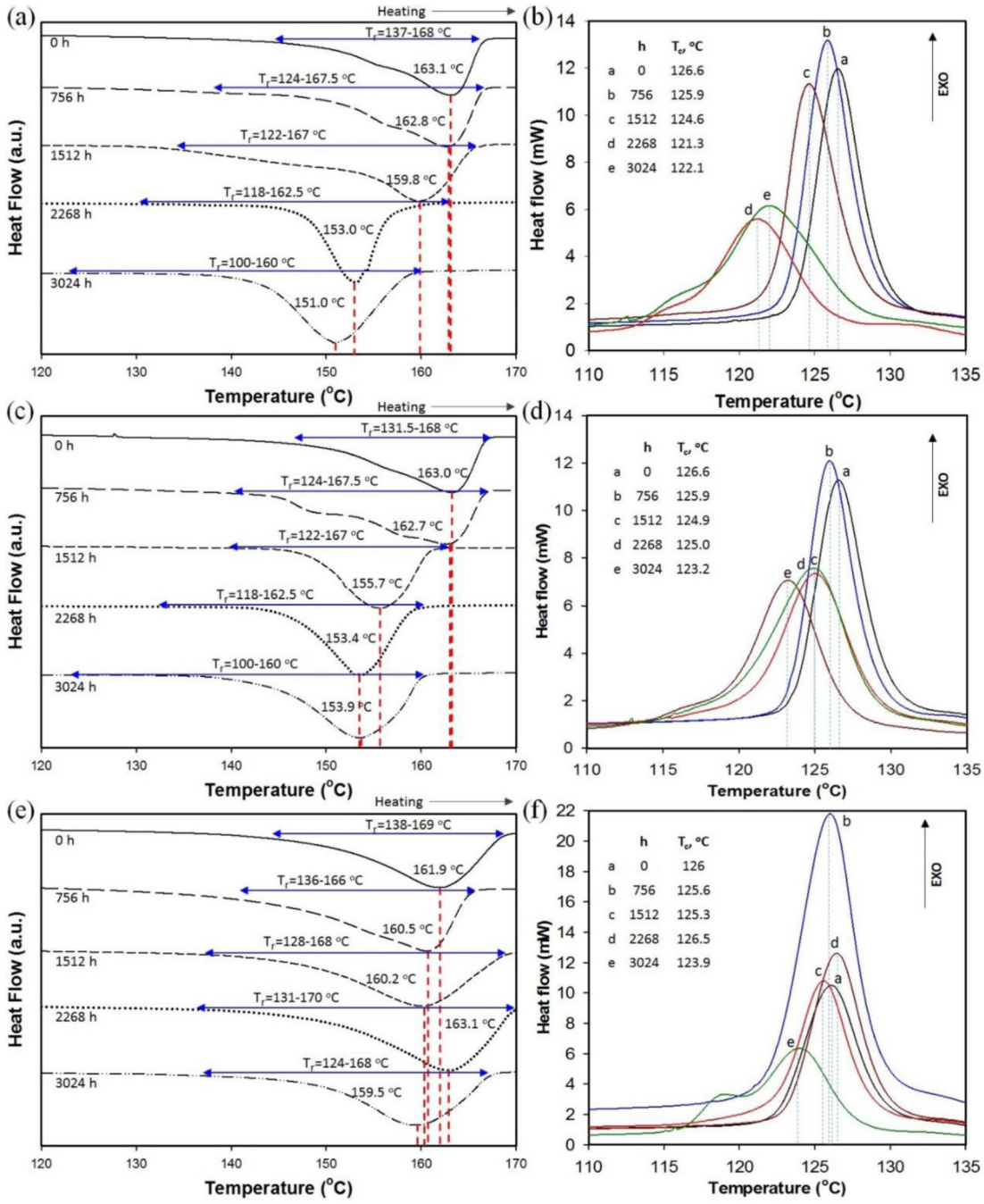

Fig. 7.

Representative DSC thermograms of unfilled PP-MWCNT for selected aging times showing: (a) melting and (b) recrystallization temperatures of PP41, (c) melting and (d) recrystallization temperatures of PP42, and (e) melting and (f) recrystallization temperatures of PP43.

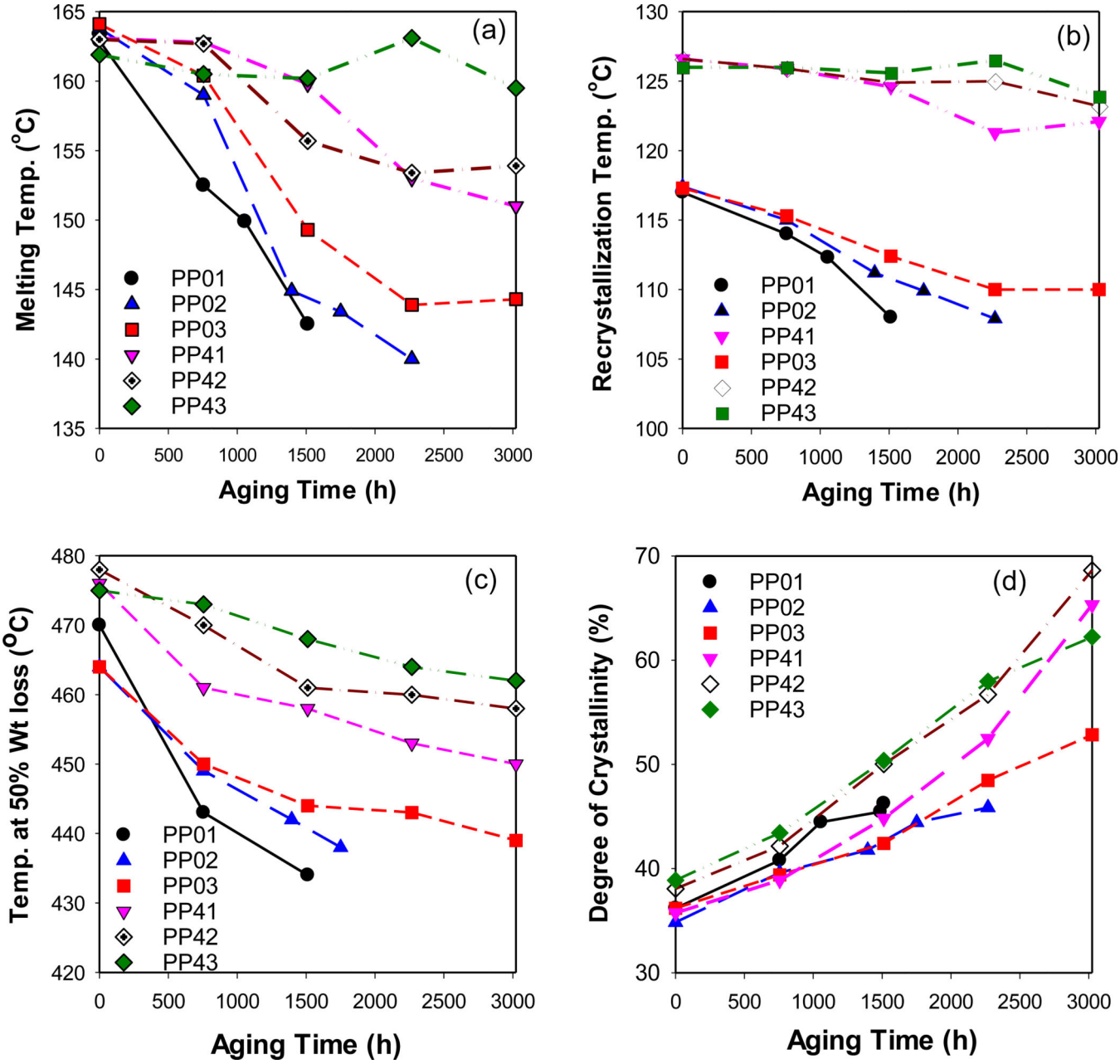

Fig. 8.

Changes in thermal properties of aged unfilled PP and PP-MWCNT composites showing the effects of aging time on, (a) melting temperature, (b) recrystallization temperature, (c) temperature of 50% weight loss, and (d) estimated the degree of crystallization.

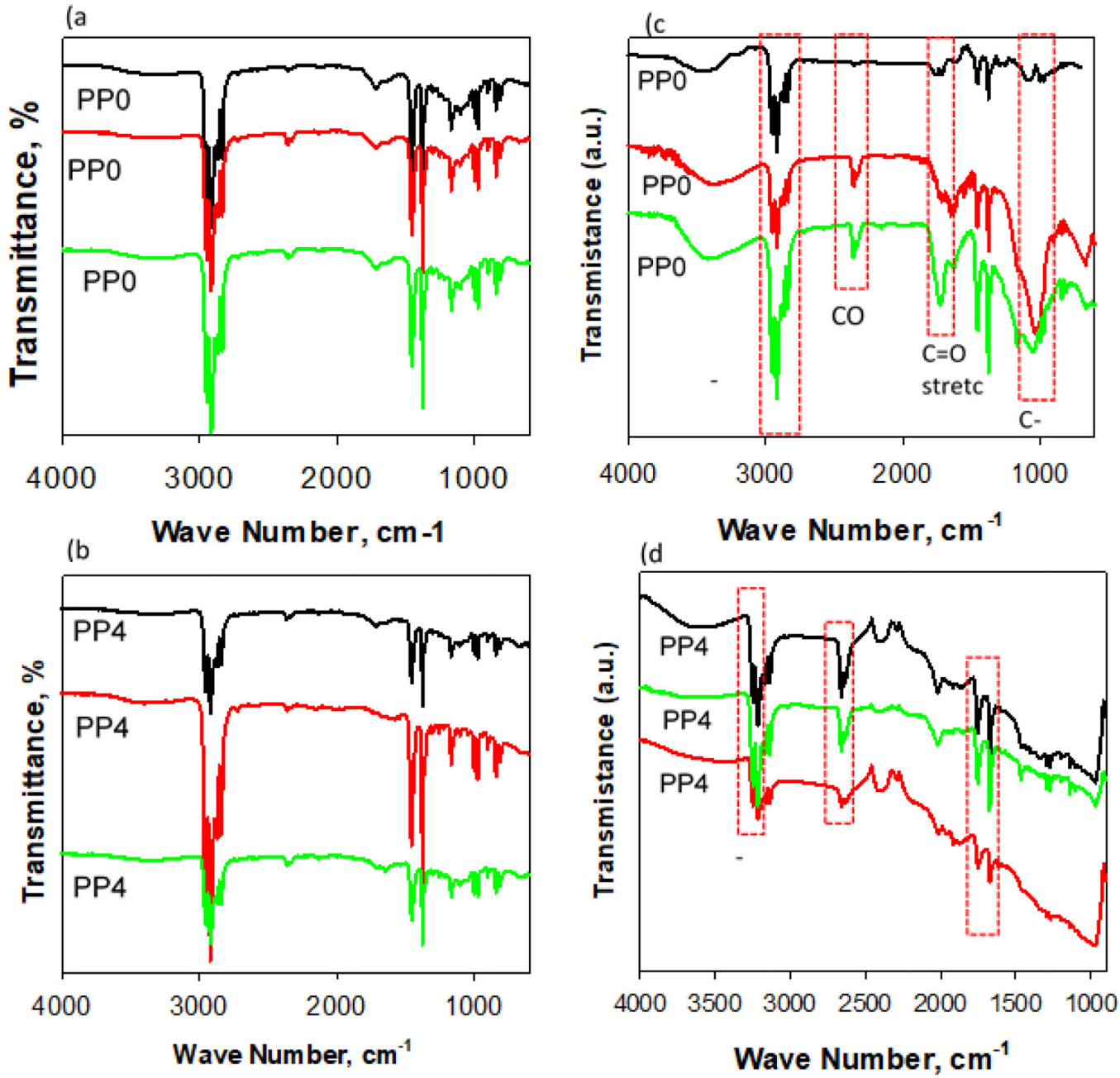

Fig. 9.

FT-IR analysis of pristine samples of (a) PP and (b) PP-MWCNT composite, and aged (c) PP and (d) PP-MWCNT composite.

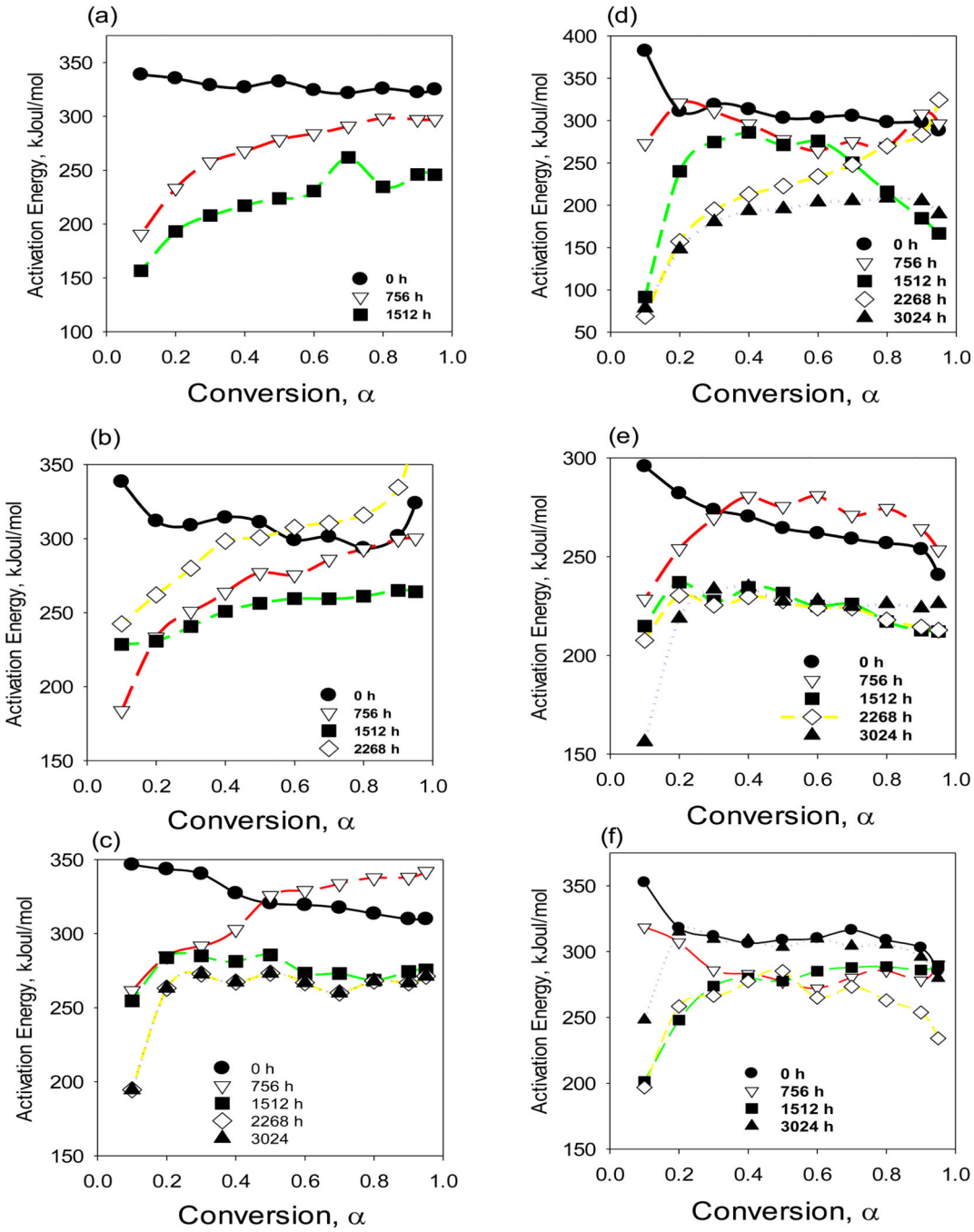

Fig. 10.

Activation energy dependencies obtained by isoconversional analysis of TGA data for pristine and aged PP with thickness (a) PP01 (L = 0.25 mm), (b) PP02 (L = 0.39 mm), and (c) PP03 (L = 0.69 mm), and PP-MWCNT composites with thickness (d) PP41 (L = 0.35 mm), (e) PP42 (L = 0.50 mm), and (f) PP43 (L = 2.27 mm).

Table 1.

Prepared films of PP and PP-MWCNT nanocomposite.

Sample	Thickness (mm)	MWCNT (%)
PP01	0.25 ± 0.01	0
PP02	0.39 ± 0.02	0
PP03	0.69 ± 0.04	0
PP41	0.35 ± 0.03	4
PP42	0.50 ± 0.01	4
PP43	2.07 ± 0.06	4

Table 2.

Experimental conditions for solar aging of PP and PP-MWCNT composite samples.

Parameter	Condition
A cycle of weathering	120 min (sunshine: 108 min and rain: 12 min)
Humidity	8–20% for Sunshine and over 60% for Rain
Solar light irradiation	700 W/m^2
Wavelength of solar light	300–800 nm
Chamber Temperature	33–37°C
Black Substance Temperature	65°C

Table 3.

Sample aging time and converted real solar exposure time for the aging study.

Aging time	Total solar radiant (MJ/m2)	Real exposure time (Month)
756 h	1909.5	3.5
1512 h	3811.4	6.9
2268 h	5726.6	10.4
3024 h	7620.4	13.9

Table 4.

Experimental Setting of thermogravimetric and differential scanning calorimetry.

TGA		**DSC**	
Instrument:	Perkin Elmer Pyrus 7 TGA	Instrument:	TA Q2000 DSC
Sample Size:	~3.0 mg	Sample Size:	~3.0 mg
Sample Pan:	Standard Aluminum Pan	Sample Pan:	Aluminum
Temperature Range:	30–800 C	Temperature Range:	90–180 C
Scanning Rate:	10–50 °C/min	Rate of Heating or Cooling:	10 °C/min
Purge Gas and Rate:	N_2 at 20 mL/min	Purge Gas and Rate:	N_2 at 20 mL/min

Table 5.

Melting temperature and crystallization temperature of aged PP and PP-MWCNT composites.

Average time (h)	Melting Temperature (°C)						Crystallization Temperature (°C)					
	PP01	PP02	PP03	PP41	PP42	PP43	PP01	PP02	PP03	PP41	PP42	PP43
0	162.9	163.8	164.1	163.1	163.0	161.9	117.0	117.4	117.3	126.6	126.6	126.0
756	152.5	162.8	160.4	162.8	162.7	160.5	114.0	115	115.3	125.9	125.9	126.0
1512	142.5	144.9	149.3	159.8	155.7	160.2	108.1	111.2	112.4	124.6	124.9	125.6
2268	-	140.0	143.9	153.0	153.4	163.1	-	107.9	110.0	121.3	125.0	126.5
3024	-	-	144.3	151.0	153.9	159.5	-	-	110.0	122.1	123.2	123.9